

## PAPER

# A Cross-Regional Cost Collaborative Optimization Model Based on a BIM Lightweight Engine and Mobile Edge Computing

Yian Zhou()

Hunan Vocational  
College of Engineering,  
Changsha, China

[yian\\_zhou994@sina.com](mailto:yian_zhou994@sina.com)**ABSTRACT**

With the rapid development of building information modeling (BIM) technology, its application in construction projects has become widespread, particularly in the collaborative work during the design, construction, and operation phases. However, traditional BIM models, due to their large data volume and complex structure, present significant challenges in data transmission and real-time processing during cross-regional collaboration. Meanwhile, mobile edge computing (MEC), as an emerging computational paradigm, reduces data transmission latency and enhances processing efficiency by deploying computing and storage resources at the network edge. The integration of a BIM lightweight engine and MEC offers a more efficient solution for cross-regional cost collaboration. While previous studies have explored the combination of BIM with cloud and edge computing, most have focused on single-region scenarios, with the lightweight methods for BIM data and MEC deployment for cross-regional collaboration still lacking efficiency and practicality. Furthermore, existing optimization algorithms often fail to fully address the unique demands of cross-regional collaboration, leading to suboptimal overall performance. To address these issues, a cross-regional cost collaborative optimization model based on the BIM lightweight engine and MEC was proposed in this study. The main content of this study includes a) the design of a BIM lightweight engine based on point cloud compression, which improves data transmission efficiency through efficient compression techniques; b) the investigation of the MEC server deployment strategy in cross-regional cost collaborative scenarios, optimizing the distribution and scheduling of computational resources; and c) the development of a cross-regional cost collaborative optimization method based on an improved genetic algorithm to enhance the intelligence and efficiency of resource scheduling. This research provides not only a new theoretical framework for the integration of BIM and MEC but also technical support for cross-regional collaborative optimization in practical engineering.

**KEYWORDS**

building information modeling (BIM), lightweight engine, mobile edge computing (MEC), cross-regional collaboration, cost optimization, genetic algorithm

Zhou, Y. (2025). A Cross-Regional Cost Collaborative Optimization Model Based on a BIM Lightweight Engine and Mobile Edge Computing. *International Journal of Interactive Mobile Technologies (iJIM)*, 19(7), pp. 83–96. <https://doi.org/10.3991/ijim.v19i07.54977>

Article submitted 2024-12-08. Revision uploaded 2025-02-03. Final acceptance 2025-02-18.

© 2025 by the authors of this article. Published under CC-BY.

## 1 INTRODUCTION

With the widespread application of building information modeling (BIM) technology, significant improvements have been made in the information management levels across the design, construction, and maintenance phases of the construction industry [1–4]. However, traditional BIM models, due to their large data volumes and high complexity, present substantial challenges in data transmission and processing [5–7]. This is especially true for cross-regional collaborative projects, where teams in different locations need to share and update BIM models in real-time, raising the demands on data transmission efficiency and timeliness [8]. Meanwhile, mobile edge computing (MEC), as an emerging computational paradigm, has been shown to reduce data transmission latency and improve computing efficiency by distributing computational resources at the network edge [9–12]. Therefore, the integration of BIM technology with MEC is expected to play a crucial role in cross-regional cost collaboration.

In construction project cost management, achieving efficient cross-regional collaboration is of great significance for controlling costs, optimizing resource allocation, and enhancing work efficiency [13–16]. By incorporating BIM lightweight engines and MEC, the bottlenecks in data transmission and real-time processing can be effectively addressed, thereby improving the collaborative efficiency of cross-regional teams. This integration not only contributes to reducing project costs and shortening construction timelines but also enhances engineering quality and project management, thus facilitating the digital transformation and intelligent development of the construction industry.

Despite some attempts to integrate BIM with cloud computing and edge computing, several limitations remain [17–22]. Firstly, traditional BIM data lightweighting methods have shortcomings in both compression efficiency and data integrity, failing to meet the demands for efficient transmission and real-time processing. Secondly, most existing MEC deployment strategies are focused on single-region scenarios and do not adequately address the complexity and dynamics of cross-regional collaborative settings. Finally, current optimization algorithms, when solving resource allocation and task scheduling problems, often overlook the unique requirements of cross-regional collaboration, resulting in limited optimization effectiveness.

A cross-regional cost collaborative optimization model that combines a BIM lightweight engine with MEC was proposed in this study, consisting of three main components. First, a BIM lightweight engine based on point cloud compression was designed, significantly reducing the data volume of BIM models through efficient data compression techniques, thereby improving transmission and processing efficiency. Second, the MEC server deployment strategy for cross-regional cost collaborative optimization scenarios was studied, aiming to optimize the distribution of computational resources and enhance the real-time processing and reliability of data. Finally, an improved genetic algorithm-based cross-regional cost collaborative optimization method was introduced, further enhancing collaboration efficiency and optimization outcomes through intelligent resource allocation and task scheduling. This research provides not only new theoretical insights for the integration of BIM and MEC but also substantial practical support for improving the efficiency and effectiveness of cross-regional cost collaboration.

## 2 BIM LIGHTWEIGHT ENGINE BASED ON POINT CLOUD COMPRESSION

### 2.1 Point cloud compression based on architectural geometric features

Three-dimensional point cloud data of buildings typically includes a large amount of geometric information, such as the spatial locations, shapes, and dimensions of structural elements such as walls, windows, door frames, and floors. These data exhibit strong regularities and spatial correlations. By analyzing the geometric features of the building, adaptive compression of point cloud data can be achieved. Unlike traditional point cloud compression methods, point cloud compression based on architectural geometric features does not merely rely on simple coordinate compression; instead, it utilizes the specific geometric forms of building structures to simplify and reconstruct the data, preserving key architectural information. This reduces redundant data and ensures that the compressed data, when decompressed, can effectively reflect the spatial structure of the building.

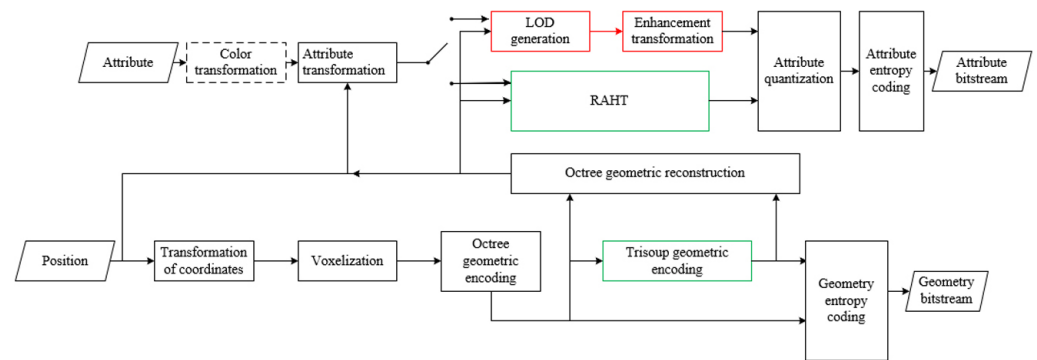


Fig. 1. Point cloud compression framework based on architectural geometric features

Figure 1 illustrates the point cloud compression framework based on architectural geometric features. In practical applications, the point cloud compression method based on architectural geometric features primarily involves parameterized modeling of the building's geometric characteristics, with various encoding methods applied to process the geometric information. First, key geometric features such as planes, curves, and angles are extracted by analyzing the primary geometric shapes of the building. These features are then converted into more compact parameters for encoding. Additionally, point cloud compression based on architectural features typically combines spatial coordinate transformation and region segmentation strategies, transforming the building's complex three-dimensional point cloud data into a more concise form with minimal information loss. Let the world coordinate system be denoted as  $A_v^{ORG}$ , the number of input point cloud points as  $V$ , the internal coordinate system as  $A_v$ , the offset variable as  $S = (MINa_v^{ORG}, MINb_v^{ORG}, MINc_v^{ORG})$ , and the quantization parameter as  $t$ . The conversion formula is as follows:

$$A_v = (A_v^{ORG} - S)/t \quad (1)$$

In the process of point cloud compression based on architectural geometric features, voxelization of the point cloud is a crucial step for subsequent octree encoding. This operation is not only essential for removing redundant points but also for optimizing the data by exploiting the inherent geometric rules of the building.

After quantization, these geometric elements can be converted into more compact voxel data, preserving key architectural information while eliminating unnecessary details. This process also allows the merging of attribute values in adjacent voxels, ensuring that each voxel represents a meaningful spatial location while avoiding redundancy caused by excessive attribute details.

Octree encoding utilizes the spatial features of the building to construct a bounding box, recursively subdividing the space into eight sub-regions based on the distribution of the point cloud. This method is particularly suitable for scenarios where the point cloud data in building structures is densely distributed, such as in planar structures like walls, windows, or columns. It enables the compact storage of geometric information within a small space. When the distribution of building point cloud data is sparser, the octree increases the number of subdivision levels, which in turn requires more bits to represent the data of each point. Furthermore, certain areas within a building may contain isolated points due to the complexity or richness of the architectural structure, which increases the subdivision levels and bit count of the octree, thus affecting encoding efficiency. To address this issue, a direct encoding mode was adopted for handling these isolated points. With direct encoding, the coordinates and attribute information of isolated points can be represented more concisely, thus reducing the generation of redundant data. Additionally, intra-frame prediction, as a compression optimization strategy, was employed. By referencing the already encoded neighboring information, the occupancy of the current node was predicted, thereby reducing unnecessary encoding data.

In point cloud compression driven by architectural geometric features, intra-frame prediction effectively utilizes the geometric rules and structural relationships of the building to minimize redundancy during the encoding process. This not only improves compression efficiency but also reduces the consumption of storage and computational resources while retaining critical building information. Specifically, the occupancy status of the current eight child nodes  $TV_{l \in [0,7]}$  was calculated by selecting 26 neighboring information. Let the index of a child node be denoted by  $l$ , the index of the neighboring region be denoted by  $j$ , the weight of neighboring region  $j$  for child node  $l$  be denoted by  $q_{j,l}$ , and the occupancy status of neighboring region  $j$  be denoted by  $\sigma_j$ . The prediction formula is as follows:

$$SC_l = \frac{1}{26} \sum_{j=1}^{26} q_{j,l}(\sigma_j) \quad (2)$$

For dynamically acquired point cloud data, attribute information is typically represented by reflectance values, which are crucial for accurately reconstructing the surface features and material properties of the building. To minimize attribute distortion between the original and reconstructed point clouds, an accurate attribute transformation operation is required in the point cloud compression method based on architectural geometric features. In lossless geometric encoding, since no points are lost, attribute values can be directly matched and copied in the reconstructed point cloud, ensuring precise recovery of the attributes. However, for lossy geometric encoding, where point numbers may be reduced, attribute interpolation is necessary to compensate for the loss of attribute information caused by the missing points. By employing interpolation methods, attribute values can be reasonably estimated and distributed within the reconstructed point cloud, ensuring that the visual effect and geometric accuracy of the reconstructed point cloud closely match the original, thereby ensuring the accurate restoration of surface details and material properties of the building.

## 2.2 Geometric evaluation metrics for the BIM lightweight engine

In the point cloud compression-based BIM lightweight engine, the core objective of geometric evaluation metrics is to assess whether the compressed point cloud data effectively preserves the geometric features of the building and to evaluate the optimization of data volume during the compression process. Geometric quality, as an important evaluation criterion, primarily focuses on the geometric differences between the original and reconstructed point clouds. In the process of building point cloud compression, geometric quality assessment not only depends on the geometric discrepancies between the point clouds but also considers the retention of architectural geometric features. For lossy compression, even if there are some geometric errors, the geometric quality can still be considered acceptable as long as the errors have minimal impact on the building structure and do not lead to the loss of key structural features. Specifically, let  $X$  represent the original point cloud,  $Y$  represent the reconstructed point cloud, and  $r_{Y,X}$  denote the geometric error between the two. For any point  $y_u$  in the reconstructed point cloud, the nearest neighbor point  $x_k$  in the original point cloud is obtained by using the nearest neighbor search method. Let  $V_Y$  denote the number of points in the reconstructed point cloud, and the error vector  $R(u, k)$  connecting  $x_k$  and  $y_u$  be defined, with its length expressed as  $\|R(u, k)\|_2$ . The point-to-point error of the reconstructed point cloud,  $r_{Y,X}^{z2z}$ , is given by the following equation:

$$r_{Y,X}^{z2z} = \frac{1}{V_Y} \sum_{\forall y_u \in Y} \|R(u, k)\|_2^2 \quad (3)$$

Let the projection error vector along the normal vector  $V_k$ 's direction be  $R(u, k)$ , and the projection error vector is denoted as  $\hat{R}(u, k)$ . The point-to-plane error calculation formula for the reconstructed point cloud is given by:

$$r_{Y,X}^{z2o} = \frac{1}{V_Y} \sum_{\forall y_u \in Y} \|\hat{R}(u, k)\|_2^2 = \frac{1}{V_Y} \sum_{\forall y_u \in Y} (R(u, k) \cdot V_k)^2 \quad (4)$$

Let the diagonal distance of the point cloud bounding box be denoted by  $o$ . The peak signal-to-noise ratio corresponding to  $r_{Y,X}^{z2z}$  and  $r_{Y,X}^{z2o}$  can be calculated using the following equation:

$$PSNR = 10 \log_{10} \frac{3o^2}{r_{Y,X}} \quad (5)$$

Geometric compression ratio is another critical evaluation metric, primarily used to measure the ratio of the compressed data volume to the original point cloud data volume. In the BIM lightweight engine, optimizing the geometric compression ratio is significant for improving storage efficiency and transmission performance. Building point cloud data often contains a large amount of redundant information, especially in areas with flat surfaces or repetitive structures. The point cloud compression method based on architectural geometric features can effectively eliminate these redundant data, significantly reducing the data volume. By employing techniques such as octree encoding and attribute encoding, the geometric compression ratio can be further improved while maintaining geometric quality, thereby reducing the consumption of storage and computational resources. For example, areas of a building that are flat and regular can be compressed at a lower resolution, while complex building structures can be compressed at a higher resolution, balancing compression efficiency

with geometric precision. Specifically, let  $ZE$  represent the compression ratio, and  $SI_{CO}$  and  $SI_{OR}$  denote the data sizes of the encoded point cloud and the original point cloud, respectively. The compression ratio can be calculated using the following formula:

$$ZE = \frac{SI_{CO}}{SI_{OR}} \times 100\% \tag{6}$$

### 3 DEPLOYMENT OF MEC SERVERS IN CROSS-REGIONAL COST COLLABORATIVE OPTIMIZATION SCENARIOS

#### 3.1 Reference scenario

In cross-regional cost collaborative optimization scenarios, the deployment of MEC servers faces multiple challenges, particularly in cases where geographical distribution is uneven and the demand for devices varies significantly (see Figure 2). Considering the distribution characteristics of industrial equipment and wireless sensors in different regions, the deployment location of MEC servers needs to be optimized based on the distribution of mobile devices. In cross-regional scenarios, the distribution of mobile devices is often random or follows certain patterns. For instance, in some industrial parks, the distribution of sensors and equipment may exhibit a localized clustering trend, whereas in urban or rural areas, devices may be more widely dispersed. Therefore, to effectively serve these mobile devices, the deployment of MEC servers must be based on the distribution of user devices. The devices can be grouped using a Gaussian mixture clustering method, with each cluster center identified as a potential deployment location for the MEC servers. Additionally, to achieve cross-regional cost collaborative optimization, the deployment of MEC servers must take into account energy consumption and network bandwidth constraints. Communication demands between devices in different regions may vary significantly, and excessive remote communication can result in high latency and energy consumption. Consequently, when deploying MEC servers, the transmission power of each device must be reasonably constrained to avoid unnecessary energy waste caused by long-distance communication. Specifically, the geographical distribution of devices is represented as a set  $U = \{u_1, u_2, \dots, u_k, \dots, u_j\}$ . The cluster centers are then treated as potential deployment locations for MEC servers, denoted as  $R = \{r_1, r_2, \dots, r_v, \dots, r_v\}$ .

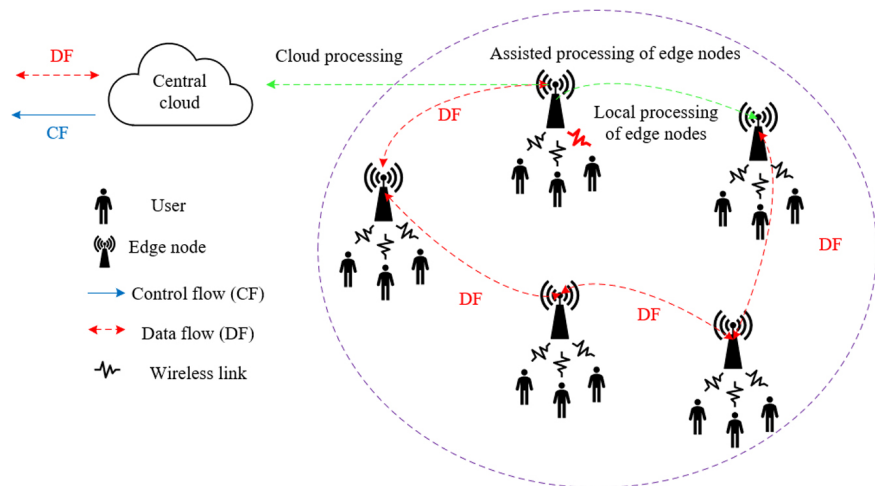


Fig. 2. Task flow diagram of the MEC network

### 3.2 System modeling

In the cross-regional cost collaborative optimization scenario, the connection between mobile devices and MEC servers is subject to a maximum distance constraint, denoted as  $F$ , and the transmission power  $o_j$  of each mobile device influences its communication quality. To achieve the cross-regional optimization objective, an energy efficiency optimization model must first be established by considering both distance and power constraints in the distribution environment of mobile devices and MEC servers. After determining the potential deployment locations for the MEC servers and communication distance constraints, the energy efficiency of each device needs to be calculated. The energy efficiency of the  $j$ -th device refers to the ratio between the amount of data it can transmit at a given transmission power and the energy it consumes. To ensure the effective utilization of network resources, an energy efficiency model for each device must be constructed. By analyzing the signal propagation characteristics of each device and considering its transmission power  $o_j$  and the distance to the MEC server, the energy efficiency of the device can be calculated. Let  $Y$  denote the system bandwidth, and the signal-to-interference-plus-noise ratio (SINR) of the  $j$ -th mobile device be denoted as  $SINR_j$ . The specific calculation formula is given as:

$$\varepsilon_j = Y \log_2(1 + SINR_j) / o_j \quad (7)$$

The SINR directly affects the reliability and rate of data transmission. Therefore, during the deployment of MEC servers, it is crucial to ensure that the SINR for each device meets the communication requirements to guarantee the system's stability and efficiency. Let  $O_{REC}(j, v)$  denote the received power of the  $j$ -th device at the  $v$ -th MEC server. The calculation formula for  $SINR_j$  is given by the following equation:

$$SINR_j = O_{REC}(j, v) / U_j = o_j \cdot h(j, v) / \left( \sum_{k \in h, k \neq v} o_j \cdot h(j, v) + \sigma^2 \right) \quad (8)$$

The reception power between each device and the MEC server is another key performance metric, as it directly affects the data transmission quality of the device. The reception power of the  $j$ -th device at the  $v$ -th MEC server can be calculated based on the device's transmission power, the distance to the MEC server, and the channel attenuation model:

$$O_{REC}(j, v) = o_j \cdot h(j, v) \quad (9)$$

In practical MEC server deployment, in addition to noise interference, signals from other devices also cause interference. The sources of interference include other devices in the same network and external wireless devices in the environment. Specifically, the interference experienced by the  $j$ -th device is denoted as  $U_j$ , and the calculation formula is given by:

$$U_j = \sum_{k \in h, k \neq v} o_j \cdot h(j, v) + \sigma^2 \quad (10)$$

In cross-regional MEC server deployment, the channel characteristics between devices and MEC servers play a decisive role. A line-of-sight (LoS) transmission channel model is used to describe the signal transmission between devices and MEC servers, particularly in open areas and between buildings. This model considers factors such as the propagation path of the signal, obstacles in the environment, and the shielding effects of buildings. By establishing an accurate LoS transmission

channel model, the signal strength, loss, and propagation delay between the device and the MEC server can be better computed. Specifically, let the LoS transmission channel between the  $j$ -th device and the  $v$ -th MEC server be denoted as  $h(j, v)$ , and the calculation formula is given by:

$$h(j, v) = \eta \cdot f(j, v)^{-\phi} \tag{11}$$

Finally, the energy efficiency of the mobile devices was maximized and defined as the objective function of the model:

$$\text{MAX} \sum_{j=1}^L \varepsilon_j \tag{12}$$

Let  $f(j, v) = \sqrt{(a_{uj} - a_{rv})^2 + (b_{uj} - b_{rv})^2}$ , where the location of the  $j$ -th device is denoted as  $(a_{uj}, b_{uj})$ , and the location of the  $v$ -th potential MEC server is denoted as  $(a_{rv}, b_{rv})$ . The distance constraint in the above expression is:

$$\text{s.t. } f(j, v) < F \tag{13}$$

The constraint on the transmission power of the device is given by:

$$o_j = O_{LRZ} / V_U \tag{14}$$

#### 4 CROSS-REGIONAL COST COLLABORATIVE OPTIMIZATION BASED ON AN IMPROVED GENETIC ALGORITHM

The aforementioned BIM lightweight engine provides geographic and functional data support for the deployment of MEC servers through precise modeling and virtualization of building information. As a form of edge computing, MEC can deploy computational and storage resources closer to the data source, thereby reducing data transmission latency and enhancing computational efficiency. In this context, an improved genetic algorithm was proposed, aimed at optimizing the deployment of MEC servers to enhance collaborative efficiency across regions and maximize the system's energy efficiency.

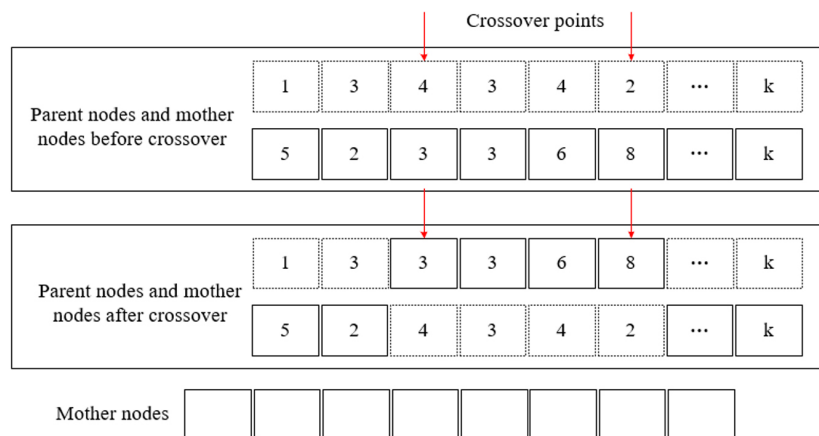


Fig. 3. Schematic diagram of the crossover operation in the improved genetic algorithm

Specifically, the improved genetic algorithm dynamically optimizes the deployment plan of cross-regional MEC servers through operations such as crossover, mutation, and selection, thus better responding to the needs of users in different regions. One of

the core innovations of the improved genetic algorithm lies in its differentiated design within the crossover operation. In traditional genetic algorithms, the purpose of the crossover operation is to generate new individuals by exchanging the genes of the parent and mother nodes, but typically, only one crossover point is used, and the dimension of gene selection is relatively limited. In contrast, in the improved genetic algorithm, multiple crossover points are designed, with each gene point offering several possible values. This provides greater flexibility in selecting potential deployment locations for MEC servers. For instance, in cross-regional MEC server deployment, the crossover operation not only exchanges genes between different individuals but also explores the deployment potential of MEC servers across different geographical regions. This design effectively enhances the search capability of the genetic algorithm, enabling a more precise identification of the optimal MEC deployment solution in terms of energy efficiency and cost in complex cross-regional scenarios. Figure 3 illustrates the crossover operation in the improved genetic algorithm.

Regarding the mutation operation, the distinction between the improved genetic algorithm and traditional genetic algorithms lies in the application of the mutation strategy. In traditional genetic algorithms, mutation is controlled by an adaptive mechanism, usually occurring in only a few individuals. However, in the improved genetic algorithm, mutation is applied to every individual, with the mutation probability and scope being flexible and adaptable based on specific conditions. In the context of cross-regional cost collaborative optimization, the increased and adjustable mutation operations allow the algorithm to explore the diversity of MEC server deployment plans more comprehensively. This is particularly crucial for optimizations related to geographical information and architectural design within the BIM engine, as it helps the system adapt to changes in the demands of different geographic areas, thereby optimizing the distribution of MEC servers and ensuring that the system can minimize cost and resource wastage while satisfying energy efficiency requirements.

## 5 EXPERIMENTAL RESULTS AND ANALYSIS

As shown in Table 1, the compression rates of the proposed algorithm before and after voxelization demonstrate that the BIM lightweight engine significantly enhances data compression efficiency through point cloud compression techniques. Specifically, the compression rate for building scan data decreased from 18.52% to 12.32%, with a difference of 6.2%, indicating the good performance of the algorithm in compressing building scan data. For indoor scene data, the compression rate dropped from 22.36% to 3.15%, with a difference of 19.21%, highlighting the algorithm's particularly remarkable effect in compressing indoor scene data. In the case of historical building data, the compression rate decreased from 23.45% to 8.26%, with a difference of 15.19%, showing the algorithm's significant advantage in compressing historical building point cloud data. These experimental results demonstrate that the proposed BIM lightweight engine effectively compresses different types of point cloud data, particularly exhibiting significant compression effects when handling high-density and complex scene data.

**Table 1.** Comparison of compression rates of the proposed algorithm before and after voxelization operation (%)

Dataset	After Operation	Before Operation	Difference
Building scan data	12.32	18.52	6.2
Indoor scene data	3.15	22.36	19.21
Historical building data	8.26	23.45	15.19

**Table 2.** Comparison of compression rates of the proposed algorithm before and after intra-frame prediction (%)

Dataset	After Prediction	Before Prediction	Difference
Building scan data	2.56	7.32	4.76
Indoor scene data	2.31	3.26	0.95
Historical building data	3.26	4.36	1.1

According to the comparison data of compression rates before and after intra-frame prediction in Table 2, the BIM lightweight engine further enhances data compression efficiency through the application of intra-frame prediction techniques. Specifically, the compression rate for building scan data decreased from 7.32% to 2.56%, with a difference of 4.76%, indicating that intra-frame prediction significantly improved the compression performance for building scan data. For indoor scene data, the compression rate reduced from 3.26% to 2.31%, with a difference of 0.95%. Although the reduction was smaller, it still demonstrates the algorithm’s ability to effectively compress indoor scene data. In the case of historical building data, the compression rate dropped from 4.36% to 3.26%, with a difference of 1.1%, further confirming the contribution of intra-frame prediction in data compression. These experimental results indicate that the intra-frame prediction technique plays an optimization role in the compression of BIM point cloud data, with particularly noticeable effects in building scan and historical building data.

Based on the data from Figure 4, which illustrates the impact of task variance on cost task completion under different methods, the BIM lightweight engine demonstrates relatively stable and superior performance. As task variance increased from 1 to 5, the completion rate of the proposed method gradually decreased from 0.915 to 0.82. However, compared to other methods, it maintained a relatively high level of performance. In comparison, the completion rates of delta encoding (from 0.9 to 0.8), entropy encoding (from 0.875 to 0.77), the Draco compression algorithm (from 0.855 to 0.755), and traditional octree encoding (from 0.78 to 0.68) exhibited more significant declines. This indicates that, when faced with tasks of varying variances, the BIM lightweight engine provides higher task completion, especially when handling tasks with high variance, where its advantage remains evident.

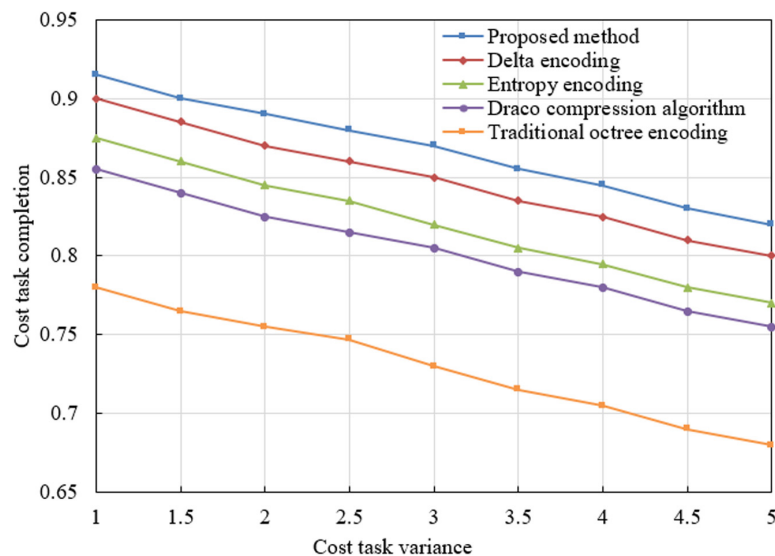


**Fig. 4.** Impact of task variance on completion of cost tasks

According to the data shown in Figure 5, which presents the local processing volume of cost tasks under different methods with varying task variance, the proposed method demonstrates superior performance, particularly in cases with higher task variance. As task variance increased from 1 to 5, the local processing volume of cost tasks using the proposed method gradually decreased from 41 to 32.5, indicating that as task complexity increased, the volume of locally processed tasks decreased. However, compared to other methods, the proposed method consistently maintained a higher task processing volume, especially when task variance was 1, where its performance was most notable. In comparison, delta encoding (from 40 to 31.8), entropy encoding (from 39.6 to 31.1), the Draco compression algorithm (from 37.5 to 29), and traditional octree encoding (from 36 to 27.5) all showed larger decreases in task processing volume. This suggests that the proposed method is more robust and effective when handling tasks with high variance.

According to the data shown in Figure 6, which presents the cloud processing volume of cost tasks under different methods with varying task variance, the proposed method demonstrates superior processing capabilities. As task variance increased from 1 to 5, the cloud processing task volume using the proposed method gradually increased from 3 to 10, indicating that the proposed method effectively allocates and schedules computing resources, thereby enhancing cloud processing capability for tasks with high variance. In comparison to other algorithms, the increase in cloud processing task volume with the rise in task variance is relatively smooth when using the proposed method. For instance, delta encoding's task volume increased from 3.4 to 10.4, entropy encoding from 4 to 11, the Draco compression algorithm from 4.4 to 11.4, and traditional octree encoding from 5 to 12. Although other methods approach or even exceed the proposed method in task volume when the task variance is large, the proposed method maintains relatively balanced and efficient cloud processing volume in cases of lower variance.

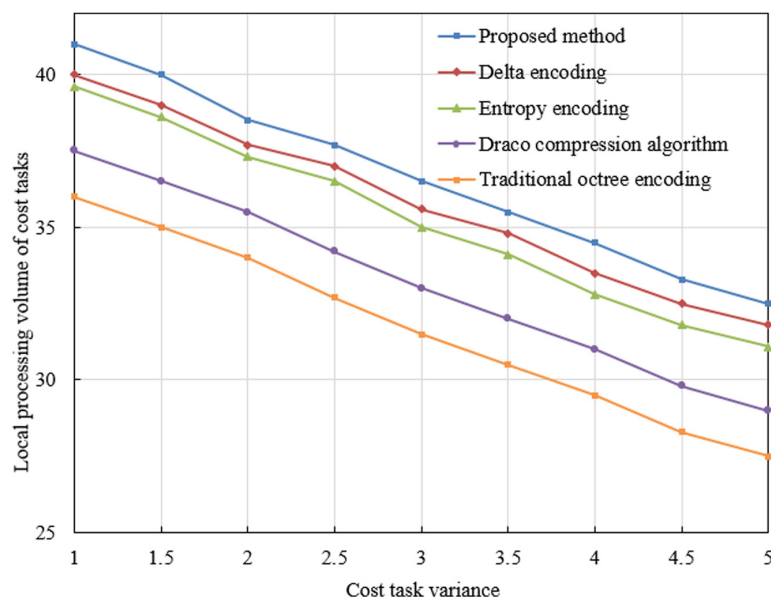


Fig. 5. Impact of task variance on the local processing volume of cost tasks

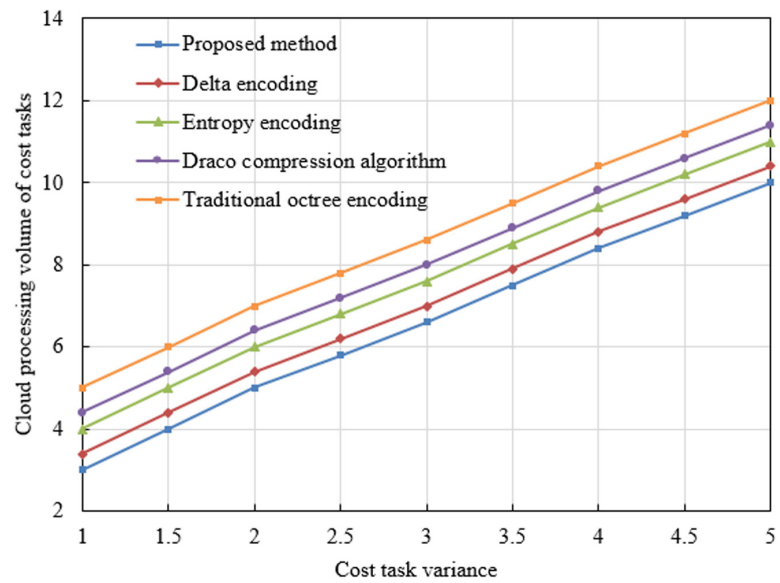


Fig. 6. Impact of task variance on cloud processing volume of cost tasks

## 6 CONCLUSION

A cross-regional cost collaborative optimization model combining the BIM lightweight engine and MEC was proposed in this study, aiming to improve the efficiency and accuracy of construction cost calculations. The core of the research involves three main aspects: first, the BIM lightweight engine significantly reduced the data volume of the BIM model through point cloud compression technology, thereby enhancing data transmission and processing efficiency; second, the deployment strategy of MEC servers was studied to optimize the allocation of computational resources, improving the timeliness and reliability of data processing; third, an improved genetic algorithm was introduced to perform intelligent resource scheduling and task allocation, optimizing cross-regional collaborative computation. Experimental results indicate that the proposed method maintains more stable task processing volumes in both cloud and local environments as task variance increases, particularly exhibiting higher efficiency and robustness under high variance conditions. Compared to other compression algorithms, the proposed method demonstrates greater adaptability and advantages across different task scenarios.

This research holds considerable practical value. First, through the BIM lightweight technology, the burden of data storage and transmission was reduced, making it suitable for large and complex construction projects. Second, the deployment and resource optimization of MEC servers enhanced the timeliness and reliability of cross-regional cost calculations. Finally, intelligent task scheduling and optimization improved the utilization efficiency of computing resources, reducing computational costs. However, there are certain limitations in the proposed method. First, the computational complexity of the task scheduling algorithm is relatively high, which may introduce computational pressure in large-scale tasks. Second, the MEC deployment strategy requires further optimization according to different engineering scenarios. Lastly, the compatibility and compression effectiveness of the BIM data compression method still need improvement.

## 7 REFERENCES

- [1] A. S. Ali, N. Zakaria, and U. K. Zolkafli, "Building operation and maintenance: A framework for simplified building information modeling (BIM) digital mobile application," *International Journal of Interactive Mobile Technologies (ijIM)*, vol. 15, no. 20, pp. 146–160, 2021. <https://doi.org/10.3991/ijim.v15i20.23753>
- [2] O. Olughoyega, "BIM leadership theory for organisational BIM transformation," *Frontiers in Built Environment*, vol. 8, 2022. <https://doi.org/10.3389/fbuil.2022.1030403>
- [3] M. Ghanbari, D. Zolfaghari, and Z. Yadegari, "Mitigating construction delays in Iran: An empirical evaluation of building information modeling and integrated project delivery," *Journal of Engineering Management and Systems Engineering*, vol. 2, no. 3, pp. 170–179, 2023. <https://doi.org/10.56578/jemse020304>
- [4] T. Funtík, P. Makýš, M. Ďubek, J. Erdélyi, R. Honti, and T. Cerovšek, "The status of building information modeling adoption in Slovakia," *Buildings*, vol. 13, no. 12, p. 2997, 2023. <https://doi.org/10.3390/buildings13122997>
- [5] F. A. Qutaiba, S. M. Omaran, and R. S. Abd Ali, "Integrate building information modeling (BIM) and occupant characteristics simulator to assess the effectiveness of emergency requirements," *International Journal of Safety and Security Engineering*, vol. 14, no. 1, pp. 37–46, 2024. <https://doi.org/10.18280/ijssse.140104>
- [6] X. Liao, C. Y. Lee, and H. Y. Chong, "Contractual practices between the consultant and employer in Chinese BIM-enabled construction projects," *Engineering, Construction and Architectural Management*, vol. 27, no. 1, pp. 227–244, 2019. <https://doi.org/10.1108/ECAM-02-2019-0110>
- [7] H. A. J. Kazem and D. A. Al-Kazzaz, "Modelling design standards for Iraqi schools using building information modeling," *International Journal of Sustainable Development and Planning*, vol. 18, no. 5, pp. 1477–1487, 2023. <https://doi.org/10.18280/ijssdp.180518>
- [8] S. Zhang, Y. Tang, Y. Zou, H. Yang, Y. Chen, and J. Liang, "Optimization of architectural design and construction with integrated BIM and PLM methodologies," *Scientific Reports*, vol. 14, 2024. <https://doi.org/10.1038/s41598-024-75940-x>
- [9] J. A. Mayan, S. V. Manikathan, A. Hussain, S. Nithyaselvakumari, and A. Vinnarasi, "Clustering technique for mobile edge computing to detect clumps in transportation-related problems," *International Journal of Interactive Mobile Technologies (ijIM)*, vol. 17, no. 4, pp. 47–63, 2023. <https://doi.org/10.3991/ijim.v17i04.37801>
- [10] Y. Guo, S. Wang, A. Zhou, J. Xu, J. Yuan, and C. H. Hsu, "User allocation-aware edge cloud placement in mobile edge computing," *Software: Practice and Experience*, vol. 50, no. 5, pp. 489–502, 2020. <https://doi.org/10.1002/spe.2685>
- [11] H. Tunga, S. Kar, and D. Giri, "Intrinsic profit maximization of the offloading tasks for mobile edge computing with fixed memory capacities and low latency constraints using Ant colony optimization," *Mathematical Modelling of Engineering Problems*, vol. 9, no. 3, pp. 668–674, 2022. <https://doi.org/10.18280/mmep.090313>
- [12] R. Raghu, V. Jayaraman, J. Jayaraman, S. S. V. Nukala, and V. G. Díaz, "A multi-layered edge-secured cloud framework for healthcare monitoring in old-age homes using smart systems driven by comprehensive user interaction," *International Journal of Safety and Security Engineering*, vol. 12, no. 4, pp. 449–457, 2022. <https://doi.org/10.18280/ijssse.120405>
- [13] D. Liu, X. Zhang, C. Gao, M. Yang, and M. Li, "Cost management system of electric power engineering project based on project management theory," *Journal of Intelligent & Fuzzy Systems*, vol. 34, no. 2, pp. 975–984, 2018. <https://doi.org/10.3233/JIFS-169391>
- [14] F. Liu and J. M. Wang, "Research on project cost management model of ecological construction," *Key Engineering Materials*, vol. 480–481, pp. 1197–1200, 2011. <https://doi.org/10.4028/www.scientific.net/KEM.480-481.1197>

- [15] J. Dai and D. Ke, “Cost early-warning model system of large-scale construction project,” *Computational Intelligence and Neuroscience*, vol. 2022, pp. 1–10, 2022. <https://doi.org/10.1155/2022/3541803>
- [16] H. Haaskjold, B. Andersen, and J. A. Langlo, “Dissecting the project anatomy: Understanding the cost of managing construction projects,” *Production Planning & Control*, vol. 34, no. 2, pp. 117–138, 2023. <https://doi.org/10.1080/09537287.2021.1891480>
- [17] R. Zheng, J. Jiang, X. Hao, W. Ren, F. Xiong, and Y. Ren, “bcBIM: A blockchain-based big data model for BIM modification audit and provenance in mobile cloud,” *Mathematical Problems in Engineering*, vol. 2019, no. 1, pp. 1–13, 2019. <https://doi.org/10.1155/2019/5349538>
- [18] I. Mutis and I. Mehraj, “Cloud BIM governance framework for implementation in construction firms,” *Practice Periodical on Structural Design and Construction*, vol. 27, no. 1, p. 04021074, 2022. [https://doi.org/10.1061/\(ASCE\)SC.1943-5576.0000652](https://doi.org/10.1061/(ASCE)SC.1943-5576.0000652)
- [19] J. Du, R. Liu, and R. R. Issa, “BIM cloud score: Benchmarking BIM performance,” *Journal of Construction Engineering and Management*, vol. 140, no. 11, p. 04014054, 2014. [https://doi.org/10.1061/\(ASCE\)CO.1943-7862.0000891](https://doi.org/10.1061/(ASCE)CO.1943-7862.0000891)
- [20] E. Alreshidi, M. Mourshed, and Y. Rezgui, “Requirements for cloud-based BIM governance solutions to facilitate team collaboration in construction projects,” *Requirements Engineering*, vol. 23, pp. 1–31, 2018. <https://doi.org/10.1007/s00766-016-0254-6>
- [21] E. Mengiste, B. Garcia de Soto, and T. Hartmann, “Automated integration of as-is point cloud information with as-planned BIM for interior construction,” *International Journal of Construction Management*, vol. 24, no. 2, pp. 137–150, 2024. <https://doi.org/10.1080/15623599.2023.2211487>
- [22] E. Alreshidi, M. Mourshed, and Y. Rezgui, “Factors for effective BIM governance,” *Journal of Building Engineering*, vol. 10, pp. 89–101, 2017. <https://doi.org/10.1016/j.jobbe.2017.02.006>

## 8 AUTHOR

**Yian Zhou** is currently affiliated with the Hunan Vocational College of Engineering, which is located in Changsha, China, with the postal code 410151. As a member of this institution, Zhou is engaged in the academic and practical aspects of engineering, contributing to both the education and development of students in this field (E-mail: [yian\\_zhou994@sina.com](mailto:yian_zhou994@sina.com); ORCID: <https://orcid.org/0009-0005-6367-7080>).